

## Results

Figure 1 shows the obtained profiles. The CO profiles were Hanning smoothed two times so the velocity resolution of the displayed profiles is  $7.2 \text{ km s}^{-1}$  and the rms noise goes from  $0.01 \text{ K}$  to  $0.03 \text{ K}$  depending on the integration time and observing conditions. The velocity range on each profile is  $1,000$  to  $2,000 \text{ km s}^{-1}$  from left to right. Along the major axis we have the profiles with the lower noise. In spite of the fact that one profile is missing in the sequence (at the offset  $60''$  to the SE) the position-velocity diagram (Fig. 2b) clearly shows the velocity variation along this axis. From this diagram it is possible to determine the heliocentric velocity of the centre of the galaxy which is  $1,470 \pm 10 \text{ km s}^{-1}$  and the rotation curve (correcting for the inclination).

The differences between this central velocity and the velocities obtained from global HI profiles by Bajaja (1978) ( $1,431 \text{ km s}^{-1}$ ) and by Reif et al. (1982) ( $1,493 \text{ km s}^{-1}$ ), are consistent with the noise in the spectra. The difference with the velocity derived by Burbidge et al. (1964) from optical observations, however, is rather large ( $64 \text{ km s}^{-1}$ ). The highest velocities along the line of sight, with respect to the centre, in Figure 2b, are about  $150 \text{ km s}^{-1}$ . This value is also smaller than the highest velocities seen optically by Burbidge et al. ( $200$  to  $250 \text{ km s}^{-1}$ ). At both ends of the diagram appear features at velocities that correspond to the other side of the galaxy which would imply rotation in the opposite sense. These features are most probably due to the noise. It should be mentioned that Burbidge et al. (1964) also found strong irregularities at both sides of the centre, although neither at the same distance nor with the same velocity differences. Along the

minor axis (Fig. 2a) the velocities cover a range of about  $275 \text{ km s}^{-1}$ . This is a consequence of the steepness of the rotation curve and the width of the beam. The CO emission is asymmetrically distributed, being mainly concentrated on the SW side.

The derivation of the molecular gas mass from the areas of the profiles of Figure 1 depends on the distance to the galaxy and on the conversion factor to  $\text{H}_2$  column densities. Both contain large uncertainties. Assuming a distance of  $19 \text{ Mpc}$  as derived from the systemic velocity, corrected for the motion with respect to the Local Group, assuming a Hubble constant of  $75 \text{ km s}^{-1} \text{ Mpc}^{-1}$ , and a conversion factor of  $4 \cdot 10^{20} \text{ cm}^{-2} (\text{K km s}^{-1})^{-1}$ , the mass of the gas in the form of molecular hydrogen would be about  $3.1 \cdot 10^9 M_{\odot}$ . The mass of the neutral hydrogen estimated by Reif et al. (1982) is about  $3.6 \cdot 10^9 M_{\odot}$ , which means that the total gas ( $\text{HI} + \text{H}_2$ ) mass would be about  $6.7 \cdot 10^9 M_{\odot}$ . Assuming an inclination angle of  $45$  degrees, the highest rotational velocities, which are measured at about  $80''$  from the centre, (Fig. 2b) are of about  $212 \text{ km/s}$ . With these values it is possible to estimate roughly the total mass within that radius as about  $7.6 \cdot 10^{10} M_{\odot}$ . The ratio between the gas and the "total" mass would then be of the order of  $9\%$  if the assumed values for the parameters used in these calculations are valid.

## Acknowledgements

We are grateful to all the ESO staff members who made these observations possible.

## References

Bajaja, E.: 1978, *Publ. Dept. Astron. Universidad de Chile*, III, 55.

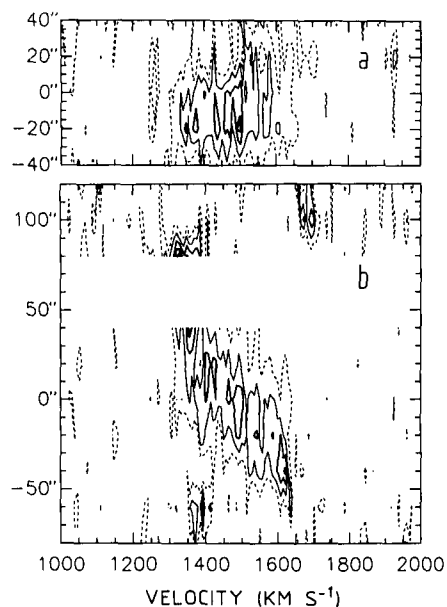


Figure 2: Position-velocity diagrams along (a) the major axis, (b) the minor axis. Velocities are heliocentric. Ordinates indicate offsets, along each axis, with respect to the centre of the galaxy. First contour lines (dashed) correspond to the level  $0.02 \text{ K}$  of antenna temperature. The contour interval is  $0.02 \text{ K}$ .

- Booth, R.S., De Jonge, M.J., Shaver, P.A.: 1987, *The Messenger* **48**, 2.  
 Burbidge, E.M., Burbidge, G.R., Rubin, V.C., Prendergast, K.H.: 1964, *Astrophys. J.* **140**, 85.  
 Elmegreen, D.M., Elmegreen, B.G.: 1982, *Astron. J.* **87**, 626.  
 Hummel, E., Jörsäter, S., Lindblad, P.O., Sandquist, A.: 1987, *Astron. Astrophys.* **172**, 51.  
 Reif, K., Mebold, U., Goss, W.M., van Woerden, H., Siegman, B.: 1982, *Astron. Astrophys. Suppl. Ser.* **50**, 451.  
 Vaucouleurs, G. de, Vaucouleurs, A. de, Corwin, H.C.: 1976, *Second Reference Catalogue of Bright Galaxies*, The University of Texas Press, Austin.

# High Resolution $\text{H}\alpha$ Spectroscopy of Nova Centauri 1986: Tracing a Transient in the Spectral Evolution

R. BANDIERA, *Osservatorio Astrofisico di Arcetri, Firenze, Italia*

P. FOCARDI, *Dipartimento di Astronomia, Università di Bologna, Italia*

We present here some preliminary results and considerations regarding high resolution spectroscopy of Nova Centauri 1986. This object was discovered on November 22.7 UT as a  $5.6 \text{ V}$  magnitude star (1), and observed by us in  $\text{H}\alpha$  two months later, when it was of about

$10$  magnitude. A considerable change in the  $\text{H}\alpha$  line profile, basically consisting in the disappearance of the original flat-top profile substituted by a more regular multicomponent profile, is clearly visible in our set of spectra, obtained monitoring the nova for nearly a week. A fitting

of the line profile by means of three gaussian components shows a narrowing of the components and a rapid fading of one of them as a function of time. This behaviour can be interpreted in terms of blobs which have been formed in a non-spherical explosion and that

were evaporating at the time of the observations.

## The Observations

The spectra were obtained during the "spare time" of an observing run with the 1.4-m CAT telescope, and the CES spectrograph equipped with the Short Camera (2) and a double-density RCA CCD. Our main goal was a search for binarity in P Cygni-type stars and red supergiants: part of the results we obtained can be found in 3, 4. The instrumental setting is of extremely high efficiency, allowing to obtain spectra of superb quality with a S/N ratio exceeding 200. The slit width was 2 arcsec on the sky, corresponding to a resolving power of nearly 40,000; the original spectra were  $\approx 50 \text{ \AA}$  wide, centred on the wavelength 6560  $\text{\AA}$ . The log of observations is reported in Table 1. Preliminary reduction (flat field correction, wavelength calibration) has been performed with the MIDAS package available at the Bologna and Arcetri Institutes. For these spectra, no absolute measurement is available to us; therefore they will be presented here, normalized to their peak value.

## The Evolution of Spectra

Spectrum # 1 appears as a flat-top spectrum, with many subcomponents and a red wing, in reasonable agreement with high-resolution spectra obtained by Pacheco (private communication) during the period 4–9 January, using the 1.4-m CAT telescope equipped with a Reticon detector. With respect to Pacheco's spectra, the  $H\alpha$  line is narrower, the red wing is less evident, while a blue component becomes visible.

After only 4 days (spectrum # 2) the  $H\alpha$  profile has changed considerably (see Fig. 1), taking on a more regular shape. Further variations are seen by a direct comparison of spectra # 2–5 (see Fig. 2, left side): the  $H\alpha$  profile is getting thinner and thinner; in the meanwhile, the component on the blue side is getting fainter and fainter.

## Derived Parameters

To give a quantitative description of the spectral evolution we fitted the profiles # 2–5 with three gaussians (two for the main component, plus one for the blue component), added to a second-order continuum: the gaussian components are labelled from 1 to 3 bluewards; for each of them  $A_i$  indicates the line amplitude,  $\lambda_i$  the central wavelength, and  $W_i$  the full width half maximum, while the continuum is approxi-

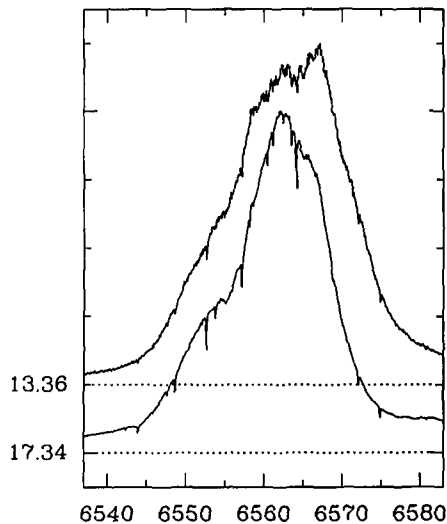


Figure 1: Comparison between Spectrum # 1 (upper spectrum) and Spectrum # 2 (lower spectrum). Both spectra are normalized; dashed lines give the zero levels for the two spectra. The dates of the observations (see Table 1) are reported on the left side.

mated by  $A + B (\lambda - 6560) + C (\lambda - 6560)^2$ .

This fit gives good results: synthesized profiles (Fig. 2, middle) reproduce the original ones well, and the residuals are limited to a few per cent (Fig. 2, right side). The main parameters of the spectra are listed in Table 2. The time dependence of the various parameters is rather clear, with the exception, for a few of them, of the Jan. 17.34 spectrum: this probably because in this spectrum the components are too blended to be separated correctly, and therefore the parameters derived from it are less accurate.

TABLE 1.

Spec- trum	Date (UT)	Exposure Time (s)
No. 1	Jan. 13.36	1200+900
No. 2	Jan. 17.34	600+600+600
No. 3	Jan. 19.35	600+600
No. 4	Jan. 20.33	600+600
No. 5	Jan. 22.36	600+600

The relative amplitude of components 1 and 2, in the main peak, remain stable with time, while component 3 fades with respect to the others with a time scale of 5 days (computed on the last 3 spectra). All components present a slight decrease of their width, as well as a slight shift of their central wavelengths with time. The continuum cannot be determined precisely: its slope seems to decrease with time, and the data are consistent with an intensity evolving as that of the former two components.

Is there any physical meaning for the three gaussian components fitted above? One could alternatively imagine that an otherwise symmetric line is partially absorbed on its blue wing, by a P Cygni-like effect. However, one would expect this effect to disappear with time, while the observed trend is the opposite. Furthermore, by fitting with gaussians the positive peak of a P Cygni line, the central wavelength of these fictitious components will shift redwards when the effect is stronger; the derived parameters, instead, go in the opposite way. Therefore we think that the line is physically composed of emission components. What we fitted with the former two components could actually be a

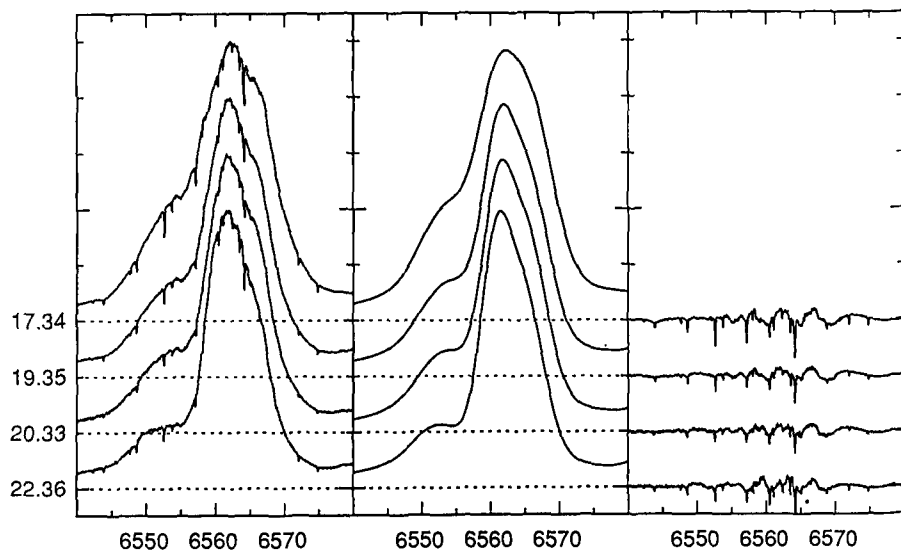


Figure 2: Comparison between Spectra # 2–5 (increasing number, i.e. increasing time, downwards). The original data are on the left; the fitted models, in the middle, are composed of 3 gaussians plus a second-order continuum; the residuals after fitting are shown on the right. All spectra are normalized; dashed lines give the zero levels of spectra. The dates of the observations (see Table 1) are reported on the left side.

TABLE 2.

Date:	Jan. 17.34	Jan. 19.35	Jan. 20.33	Jan. 22.36
$\bar{\lambda}_1$	6566.0	6565.4	6565.3	6564.7
$\bar{\lambda}_2$	6560.8	6560.9	6560.9	6560.5
$\bar{\lambda}_3$	6553.4	6554.0	6553.4	6552.5
$W_1$	7.5	7.1	6.8	6.9
$W_2$	6.6	5.3	5.2	5.0
$W_3$	8.7	9.7	9.2	8.6
$A_2/A_1$	1.01	0.98	1.06	1.04
$A_3/A_1$	0.47	0.41	0.32	0.22
$A_1/A$	4.81	5.74	6.16	6.04
$A_3/A$	2.27	2.31	2.10	1.36
$B/A$	$8.5 \cdot 10^{-3}$	$7.1 \cdot 10^{-3}$	$5.8 \cdot 10^{-3}$	$1.9 \cdot 10^{-3}$
$C/A$	$-0.9 \cdot 10^{-3}$	$-0.8 \cdot 10^{-3}$	$-1.0 \cdot 10^{-3}$	$-1.0 \cdot 10^{-3}$

unique non-gaussian component: however, the result of the two-component fit looks remarkably good.

### Discussion

It is difficult to explain the details of this line evolution by a spherically symmetrical model and, on the other hand, there is evidence for departures, in nova events, from spherical symmetry (e.g. 5, 6). In our case one could imagine that, while most of the nova shell disappeared due to dilution effects, some denser blobs began dominating the H $\alpha$  emission. The velocity dispersions of the three components are respectively 190, 140 and 250 km/s, and represent their expansion velocities.

Assuming that all blobs have similar sizes, the time scale for the fading of the line emission is inversely proportional to the blob expansion velocity, and in fact

component # 3, the broader one, gets dimmer faster than the others. Let us define  $\tau_{12}$  as the time scale for the fading of the former two components, and  $\tau_3$  as that for the latter one; since the decrease of component # 3 relative to the others is 5 days, its absolute time scale is  $\tau_3 = 1/(1/5 + 1/\tau_{12})$ . Requiring also that time scales are inversely proportional to the components' expansion velocities,  $\tau_{12}$  and  $\tau_3$  can be derived separately as, respectively, 3 and 1.9 day.

Unfortunately we do not possess absolute calibration of our spectra; anyhow, we observed that the continuum was evolving, in those days, as the components # 1 and # 2. But a rough estimate of the continuum evolution can be given by taking the decrease of the visual magnitude: by using visual magnitudes measured during the month of January (7, 8), the average decrease turns out to be 0.35 mag/day, corre-

sponding to a time scale of 3.1 day, in close agreement with our previous derivation.

A decrease in line amplitude can then be ascribed to expansion of condensations in the nova envelope; they have typically a size of  $\approx 10^{13}$  cm, much smaller than the envelope size at that time ( $\approx 5 \cdot 10^{14}$  cm); since the components are partially blended, they should be confined to the inner regions ( $\approx 10^{14}$  cm).

Therefore a way to explain the observed H $\alpha$  behaviour of Nova Centauri 1986 involves the presence of a non spherical explosion, with the formation of small condensations.

We are indebted to M. Friedjung and E. Oliva for interesting suggestions, and to J.A. de Freitas Pacheco for giving us a copy of his spectra.

### References

- (1) McNaught, R.H. 1986, *IAU Circ.* N. 4274.
- (2) Dekker, H., Delabre, B., D'Odorico, S., Lindgren, H., Maaswinkel, F., and Reiss, R. 1986, *The Messenger* **43**, 27.
- (3) Gratton, R.G., Focardi, P., and Bandiera, R. 1989, *M.N.R.A.S.*, submitted.
- (4) Bandiera, R., Focardi, P., Altamore, A., Rossi, C. and Stahl, O. 1988 *Physics of Luminous Blue Variables*, IAU Coll. No. 113, in press.
- (5) Mustel, E.R., and Boyarchuk, A.A. 1970, *Ap.Sp.Sci.* **6**, 183.
- (6) Hutchings, J.B. 1972, *M.N.R.A.S.* **158**, 177.
- (7) McNaught, R.H., Campos, J. 1987, *IAU Circ.* N. 4298.
- (8) McNaught, R.H., 1987, *IAU Circ.* N. 4315.

## The European Working Group on Chemically Peculiar Stars of the Upper Main Sequence: The First 10 Years

G. MATHYS (Genève), H. M. MAITZEN (Vienna), P. NORTH (Lausanne),  
H. HENSBERGE (Brussels), W. W. WEISS (Vienna), S. ANSARI (Vienna),  
F. A. CATALANO (Catania), P. DIDELON (Strasbourg), R. FARAGGIANA (Trieste),  
K. FUHRMANN (Göttingen), M. GERBALDI (Paris), P. RENSON (Liège),  
H. SCHNEIDER (Göttingen)

### 1. Introduction

A fraction of the B and A type stars have chemical peculiarities (CP). 4 sub-groups are recognized: CP1 or Am, CP2 or magnetic Ap (with enhanced Sr, Cr, Eu, Si lines), CP3 (or non-magnetic Ap, with Hg Mn enhanced) and CP4 (B type stars with He peculiarities, a fraction of them appear to be a hot extension of CP2).

For 10 years now, European as-

tronomers interested in the study of CP stars, and more particularly of Ap-Bp (or CP2 to CP4) stars, have gathered their efforts in a working group (WG). Many of the results obtained by members of this WG have been derived from observations obtained at ESO-La Silla. In the *Messenger* No. 34, an overview of the activity of the group during its first five years of existence was given. On the occasion of the 10th anniversary of our

WG we want to present a new report on its work with emphasis on those studies carried out during the last five years.

Beside the original research work of the various group members, a *Catalogue of CP-stars* has been compiled by P. Renson. This list was set up after a large critical survey of the literature; it contains more than 6,000 stars, half of which are CP1 (i.e. metallic line) stars. A number of remarks are provided for